Journal of Medicinal Chemistry

Article

pubs.acs.org/jmc

Discovery of Novel Bacterial RNA Polymerase Inhibitors: Pharmacophore-Based Virtual Screening and Hit Optimization

Stefan Hinsberger,[†] Kristina Hüsecken,[†] Matthias Groh,[†] Matthias Negri,[†] Jörg Haupenthal,[†] and Rolf W. Hartmann*[,†,‡]

[†]Helmholtz-Institute for Pharmaceutical Research Saarland, Department of Drug Design and Optimization, and [‡]Pharmaceutical and Medicinal Chemistry, Saarland University, Campus C2.3, 66123 Saarbrücken, Germany

Supporting Information

ABSTRACT: The bacterial RNA polymerase (RNAP) is a validated target for broad spectrum antibiotics. However, the efficiency of drugs is reduced by resistance. To discover novel RNAP inhibitors, a pharmacophore based on the alignment of described inhibitors was used for virtual screening. In an optimization process of hit compounds, novel derivatives with improved in vitro potency were discovered. Investigations concerning the molecular mechanism of RNAP inhibition reveal that they prevent the protein−protein interaction (PPI) between σ^{70} and the RNAP core enzyme. Besides of reducing RNA formation, the inhibitors were shown to interfere with bacterial lipid biosynthesis. The compounds were active against Gram-positive pathogens and revealed significantly lower resistance frequencies compared to clinically used rifampicin.

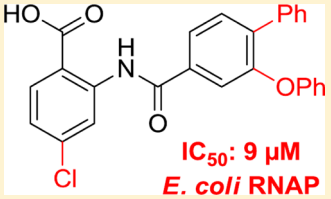

INTRODUCTION

The increasing resistance of bacteria against antibiotics has become a major public health problem.[1] Therefore, new potent antibacterial drugs are required.[2] RNA polymerase (RNAP) catalyzes the formation of RNA from a DNA template[3] and is essential for growth and survival of bacteria. It is highly conserved among various bacterial species but is different in eukaryotes.[4] Hence, inhibiting RNAP is an attractive strategy for the treatment of bacterial infections.[4]

In spite of the fact that several inhibitors of bacterial RNA polymerase are known, only rifamycins and fidaxomicin (lipiarmycin) are currently approved for clinical use.[3,5−7] Because of an increasing amount of bacterial strains resistant to rifamycins, there is an urgent need to discover new RNAP inhibitors for clinical use which should not show cross-resistance to rifamycins, especially rifampicin (Rif).

In this work, a flexible alignment of structurally similar selected synthetic molecules (**I**−**VII**) that are known to inhibit bacterial RNAP[8−12] was performed (Figure 1). The resulting pharmacophore model was subsequently used to virtually screen an in-house database. Thus, three hit compounds, containing an anthranilic acid core, were identified and experimentally validated. In the following, the compounds were optimized to improve the inhibitory profile and their mode of action was determined. Additionally, the compounds revealed good antibacterial activities.

PHARMACOPHORE-BASED VIRTUAL SCREENING AND HIT COMPOUND DISCOVERY

Seven synthetic bacterial RNAP inhibitors (**I**−**VII**) that exhibit similar structural features, although belonging to different classes and acting via different binding modes, were retrieved from literature (Figure S1, Supporting Information (SI)).[8−12] Compound **I** inhibits *Staphylococcus aureus* RNAP, but its binding site is not known.[8] **II** and **III** are described as inhibitors of *Escherichia coli* RNAP binding to a surface exposed groove at the junction of the β'-bridge helix and the β-subunit.[9] **IV**−**VI** are known to prevent the protein−protein interaction (PPI) between σ^{70} and the RNAP core enzyme.[10,11] **VII** shows structural similarity to known RNAP inhibitors but has only been described as an inhibitor of transcription and translation (TT) without any information about its mode of action.[12] We resynthesized **VII** and were able to demonstrate its inhibition of *E. coli* RNAP in vitro (SI).

I−**VII** were employed in a flexible alignment with the aim to identify the common features of these molecules. The alignment with the best similarity score was used to generate an initial pharmacophore model, which was then manually refined. The resulting model derived from these differently acting compounds is not restricted to the identification of hits binding to one special site. It should rather support the discovery of an increased number of RNAP inhibitors independent of their binding mode.

The final model consisted of four core features (two aromatic, one HBD/HBA/aromatic and one O2/anion). Besides, one accessory feature (hydrophobic) and two aromatic projections were identified (Figure 1, Figure S2, SI). The fit of each inhibitor **I**−**VII** into the pharmacophore model is depicted in Figure S3, SI. The virtual screening of an in-house database comprising approximately 2000 compounds using this pharmacophore model afforded 64 hits. A virtual hit had to match at least the core features and the aromatic projections, while the presence of the accessory feature was not mandatory.

Received: March 7, 2013
Published: October 11, 2013

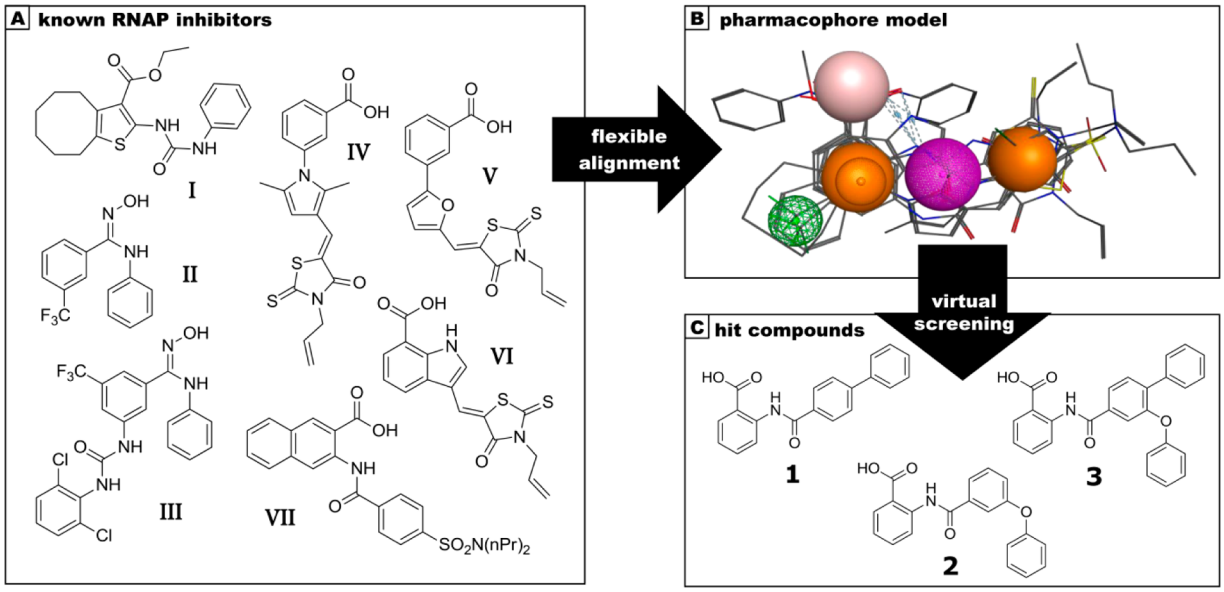

Figure 1. (A) Selected synthetic inhibitors of bacterial RNAP (**I**–**VII**) were used to perform a flexible alignment. (B) A pharmacophore model with four core features (aromatic, orange; HBD/HBA/aromatic, violet; O2/anion, rose), one accessory feature (hydrophobic, green), and two aromatic projections (one hatched orange, one hidden behind a core feature) was created and used for virtual screening. For an overlay of **I**–**VII** with the pharmacophore model, see Figure S3, SI. (C) Validated hit compounds **1**–**3** possessing an RNAP in vitro inhibition >20% at a concentration of 200 μM.

Eleven of these hit compounds originating from five different structural classes were experimentally confirmed to be active in our in vitro transcription assay[13] (>20% inhibition at 200 μM) (Figure S4, SI). Out of these, three promising compounds (**1**–**3**), containing an anthranilic acid core, were chosen for further optimization. They displayed 31% (**1**), 23% (**2**), and 100% (**3**, IC_{50} 20 μM) inhibition at 200 μM, respectively.

CHEMISTRY

The synthesis of the target compounds was carried out starting from the appropriate anthranilic acids. The methyl 2-benzamidobenzoate intermediates **1a**–**34a** were synthesized via coupling reaction with the benzoyl chloride derivatives (Scheme 1). The methyl esters were hydrolyzed to yield the target compounds. A Suzuki coupling with phenylboronic acid was performed with the appropriate brominated intermediates to obtain compounds **31** and **32**. The hydroxy substituted compound **24** was obtained from the methoxy intermediate **24a** by ether cleavage using boron tribromide.

Scheme 1. Synthetic Route to Compounds 1–34[a]

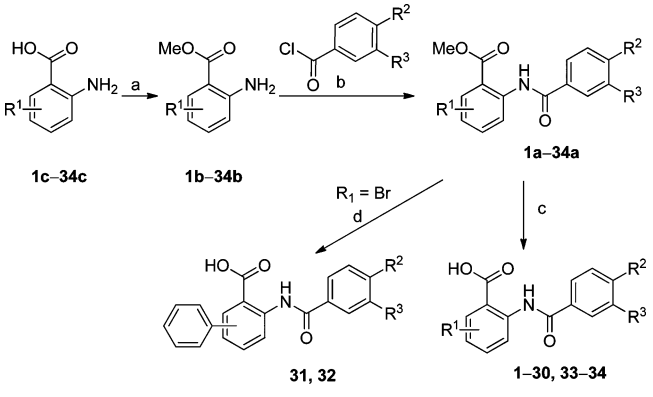

[a]Reagents and conditions: (a) $SOCl_2$, MeOH, reflux; (b) pyridine, DMAP, rt or TEA, CH_2Cl_2, rt or toluene, reflux; (c) NaOH, THF/MeOH/H_2O, rt; (d) $PhB(OH)_2$, $Pd(PPh_3)_4$, Cs_2CO_3, DME/H_2O, reflux.

RESULTS AND DISCUSSION

Compounds **1**–**3** contain a 2-benzamidobenzoic acid partial structure which perfectly fits into the pharmacophore model. In addition, the structures contain a phenyl ring in *para*- and/or a phenoxy substituent in *meta*-position, respectively, which does not correspond to any feature of the pharmacophore model. Hence, the hit compounds were reduced in size to investigate whether these lipophilic residues are necessary for activity. Although the unsubstituted 2-benzamidobenzoic acid (**4**) fits the pharmacophore model, no activity was observed for this compound. This resulted in the conclusion that the features included in the first pharmacophore model are insufficient to differentiate between active and inactive substances. To provide a remedy, two new accessory hydrophobic/aromatic features were added on the eastern side of the pharmacophore model (representing the phenyl and the phenoxy substituents) (Figure S5, SI). Using this extended model, a compound will be defined as a hit if, beside the four core features, at least one of the new accessory features is present. As the extended model is more limiting, its use should improve efficacy and reduce the occurrence of false positives in future screenings. An overlay of inhibitors with the extended pharmacophore model can be found in Figure S6, SI.

To explore the structure–activity relationship (SAR) around the anthranilic acid core, substituents were introduced in 4- and 5-position where the pharmacophore model contains a lipophilic accessory feature. As the most potent hit compound **3** has a relatively high molecular weight, optimization efforts were started modifying the two smaller hits **1** and **2**. For each hit, a small series was synthesized introducing 4-Cl (**6** and **7**), 5-F (**11** and **12**), 5-Br (**16** and **17**), and 4,5-dimethoxy (**19** and **20**) substituents. The introduction of these substituents

dx.doi.org/10.1021/jm400485e | J. Med. Chem. 2013, 56, 8332–8338

resulted in an increased in vitro activity, especially for the compounds with 4-Cl (**6** and **7**) and 5-Br (**16** and **17**) substituents. Aside from that, most 4-phenyl and 3-phenoxy compounds displayed very similar activities. To investigate whether the oxygen of the phenylether group has a beneficial effect as HBA, we synthesized compound **18** containing a 3-benzyl instead of the 3-phenoxy substituent. The removal of the oxygen did not affect the potency, indicating that a HBA is not necessary for in vitro activity. Therefore we regarded it as sufficient to continue the SAR studies introducing further substituents into the 4-phenyl series.

To determine which kind of substituents could improve activity, substituents differing in electronic properties and lipophilicity were introduced in 5-position. The incorporation of the lipophilic, electron withdrawing chloro substituent resulted in the most potent compound **8** while a hydrophilic and electron donating hydroxy group (**24**) decreased activity in comparison to **1**. Introduction of a lipophilic and electron donating substituent (**30**, CH_3) or a hydrophilic electron withdrawing substituent (**26**, CN) was tolerated and led to moderately active compounds.

In a next step, the best position for a substitution at the anthranilic acid moiety was determined. Considering the good activity of chloro compound **8**, especially lipophilic, electron withdrawing substituents in different positions of the anthranilic acid moiety were introduced. A chloro substituent in 3-position (**5**) led to a total loss of activity. Similar results were found for the chloro, fluoro, and methoxy substituents in 6-position (**9**, **13**, **23**) (Table 1). As expected, the introduction of an electron donating methoxy substituent in 4- and 5-position afforded only a moderate improvement of activity. In contrast all the compounds bearing a lipophilic, electron withdrawing substituent in 4- or 5- position (**6**, **8**, **10**, **11**, **14**, **16**, **25**, **27**–**29**) possess a highly improved in vitro potency. Especially the introduction of a large lipophilic phenyl substituent in 4- or 5-position generated very potent inhibitors of RNAP (**31**, 14 μM; **32**, 13 μM). Interestingly, almost no difference in activity was observed between compounds with a substituent in 4-position and compounds with the same substituent in 5-position (**6** and **8**, **10** and **11**, **14** and **16**, **27**, and **28**).

From these results, it is obvious that especially lipophilic electron withdrawing substituents attached to the anthranilic acid core in 4- or 5-position are favorable, whereas substituents in 3- or 6-position strongly reduce the in vitro activity.

After all, the acquired SAR information of the anthranilic acid core was used for the optimization of **3**. As it was not eligible to make the compounds too large and lipophilic, only F and Cl were introduced (**33** and **34**). As expected, these modifications had a beneficial effect on the activity and afforded the best in vitro compound of this series (**34**, 9 μM).

As the pharmacophore model is not restricted to one special binding site, it remains to be clarified where our compounds bind to RNAP. Comparing the structures of the optimized hit compounds and the inhibitors **I**–**VII**, used to create the pharmacophore model, it becomes apparent that the new compounds are very similar to **VII**. This suggests that **VII** and our compounds are likely to interact with the same RNAP site. However, the binding mechanism of **VII** is not known.

One possible mechanism of action could be the inhibition of the PPI between σ^{70} and the RNAP core enzyme because this has been demonstrated to be the way compounds **IV**–**VI** function.[10,11] Hence, selected compounds (**3**, **9**, **14**, **28**, **32**, **34**) as well as TT inhibitor **VII** were tested in an ELISA-based RNAP assembly assay.[14] Rif and **V** were used as negative and positive controls, respectively. In contrast to Rif and inactive compound **9**, inhibitors **3**, **14**, **28**, **32**, **34**, and **VII**, which had been active in the transcription assay, inhibit PPI between σ^{70} and the RNAP core enzyme to a similar extent as positive control **V** (Table 2).

Inhibitors acting via such a mechanism would be expected to show a stronger effect in a σ^{70}-dependent transcription assay using holo enzyme than in a σ^{70}-independent transcription assay with core enzyme. To further confirm PPI interruption as

Table 1. Inhibitory Activity against *E. coli* RNA Polymerase in Vitro and Antibacterial Activity

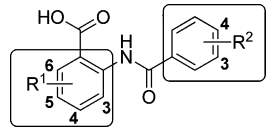

compd	R^1	R^2	IC_{50} or % inhibition of *E. coli* RNAP[a]	MIC *E. coli TolC* (μg/mL)[b]
1	H	4-Ph	31%	13
2	H	3-OPh	23%	9
3	H	3-OPh, 4-Ph	20 μM	13
4	H	H	ni	>100
5	3-Cl	4-Ph	ni	55
6	4-Cl	4-Ph	37 μM	3
7	4-Cl	3-OPh	44 μM	3
8	5-Cl	4-Ph	46 μM	2
9	6-Cl	4-Ph	ni	57
10	4-F	4-Ph	98 μM	4
11	5-F	4-Ph	138 μM	7
12	5-F	3-OPh	98 μM	5
13	6-F	4-Ph	14%	34
14	4-Br	4-Ph	28 μM	2
15	4-Br	3-OPh	34 μM	3
16	5-Br	4-Ph	31 μM	3
17	5-Br	3-OPh	34 μM	3
18	5-Br	3-CH_2Ph	37 μM	2
19	4-,5-OMe	4-Ph	35%	19
20	4-,5-OMe	3-OPh	154 μM	6
21	4-OMe	4-Ph	162 μM	9
22	5-OMe	4-Ph	52%	8
23	6-OMe	4-Ph	ni	58
24	5-OH	4-Ph	17%	31
25	4-NO_2	4-Ph	36 μM	>25
26	5-CN	4-Ph	23% @ 50 μM	7
27	4-CF_3	4-Ph	27 μM	5
28	5-CF_3	4-Ph	28 μM	2
29	5-OCF_3	4-Ph	31 μM	4
30	5-Me	4-Ph	139 μM	7
31	4-Ph	3-OPh	14 μM	8
32	5-Ph	3-OPh	13 μM	2
33	4-F	3-OPh, 4-Ph	13 μM	>25
34	4-Cl	3-OPh, 4-Ph	9 μM	>25
Rif			0.03 μM	10
Myx[c]			0.35 μM	1

[a]IC_{50} value (SD <20%) or percentage inhibition at 200 μM (SD <40%); Data represent the mean values of at least three experiments. ni: no inhibition. [b]Minimum inhibitory concentration; data represent the mean values of at least two independent experiments (three for MIC <10 μg/mL). [c]Myx: myxopyronin B.

dx.doi.org/10.1021/jm400485e | J. Med. Chem. 2013, 56, 8332–8338

Table 2. Results of the ELISA-Based Assembly Inhibition Assay and the Core/Holo Transcription Assay

compd	assembly inhibition σ^{70}/RNAP core (ELISA) (IC_{50})[a]	inhibition of RNAP holo (IC_{50})[a]	inhibition of RNAP core (IC_{50})[a]	ratio[b]
Rif[c]	n.i.	27 nM	16 nM	1
V[c]	30 μM	38 μM	57 μM	2.6
VII	97 μM	52 μM	81 μM	2.6
3	41 μM	20 μM	36 μM	3.0
9	ni	nd	nd	
14	68 μM	27 μM	39 μM	3.0
28	60 μM	28 μM	67 μM	4.0
32	47 μM	16 μM	27 μM	2.8
34	33 μM	7 μM	12 μM	2.9

[a] IC_{50} value (SD <20%); Data represent the mean values of at least two experiments. ni: no inhibition; for **9** inhibition <10% at 50 μM; for Rif inhibition <5% at 10 μM. nd: not determined. [b] (IC_{50} core:$holo_{compd}$/IC_{50} core:$holo_{Rif}$). The core:holo IC_{50} ratios were related to the Rif core:holo ratio. [c] Inhibition values of core/holo transcription assay by Hüsecken et al.[14]

RNAP inhibitory mechanism, we tested our compounds in both assays in parallel. Indeed, **3**, **14**, **28**, **32**, **34**, and **VII** were found to be more active in the assay using holo enzyme than in the core enzyme assay (Table 2). To normalize interassay conditions, ratios of IC_{50} values (core:holo) were calculated in relation to IC_{50} ratio (core:holo) of Rif, which was used as negative control not acting via PPI inhibition. The calculated IC_{50} ratios (core:holo) of the tested compounds are within the range of 2−4, comparable or even higher than the ratio of described PPI inhibitor **V** (Table 2). These results confirm the assumption that the mechanism of action of our compounds and TT inhibitor **VII** is the interference with the interaction between σ^{70} and RNAP core enzyme.

■ ANTIBACTERIAL ACTIVITY

For investigation of antibacterial activity, minimum inhibitory concentration (MIC) values were determined for all compounds. Two described RNAP inhibitors were used as references: Rif, which reveals a good antibacterial activity against Gram-positive and negative strains,[15−18] and the natural product myxopyronin B, only active against Gram-positive bacteria.[19] To evade effects associated with drug efflux, initial MIC tests were performed using *E. coli TolC* mutant, deficient in the AcrAB−TolC multidrug efflux system. There are several compounds possessing high antibacterial activity comparable to the reference compounds, especially **6**−**8**, **14**−**18**, **28**, and **32**, with MIC values in the range of 2−3 μg/mL. For most compounds, antibacterial activity roughly correlates with in vitro RNAP inhibition. However, for some highly potent inhibitors, compounds **25**, **33**, and **34**, bacterial growth inhibition was less than expected, a finding which possibly was caused by permeability problems.

To further explore the antibacterial profile, MIC values for *E. coli K12*, *Pseudomonas aeruginosa*, *Bacillus subtilis*, and *Staphylococcus aureus* were determined for selected compounds (**6**, **7**, **12**, **15**, **28**, **32**, **33**; Table 3). None of the tested inhibitors reduced the growth of Gram-negative strains (*E. coli K12* and *P. aeruginosa*). These results suggest that the compounds are either not able to penetrate the cell membranes of the Gram-negative bacteria or are discharged by efflux pumps. The latter mechanism is more probable considering the differences between the MIC values for *E. coli K12* and *E. coli TolC*. On the other hand, the inhibitors were in general effective against Gram-positive bacteria; especially against *Bacillus subtilis* excellent MIC values were determined.

Table 3. Minimum Inhibitory Concentration (MIC) for Selected Compounds

	MIC (μg/mL)[a]			
compd	*E. coli* K12	*PA01*[b]	*B. subtilis*	*S. aureus*
Rif[c]	7	13	5	0.02
Myx[c]	>25	>25	0.9	0.5
6	>50	>50	2	24
7	>50	>50	3	14
12	>100	>100	4	48
15	>25	>25	3	8
28	>50	>50	4	5
32	>25	>25	3	6
33	>25	>25	>25	17

[a] Minimum inhibitory concentration; Data represent the mean values of at least two independent experiments (three for MIC <10 μg/mL). [b] *P. aeruginosa*. [c] Rif, rifampicin; Myx, myxopyronin B.

It is striking that our compounds show very low MIC values comparable to the reference compounds although their RNAP inhibitory activities are less pronounced than those of the references.

To confirm the mechanism of antibacterial activity, the impact on macromolecular biosynthesis in *E. coli TolC* was examined. While exerting no appreciable effect on DNA and protein synthesis at 4 × MIC, **32** displayed an inhibition of RNA formation comparable to the clinically used RNAP inhibitor Rif (Figure 2). In addition, a strong decrease in lipid

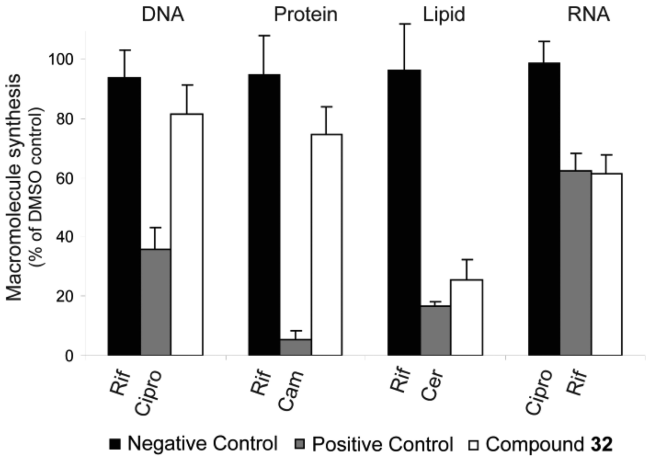

Figure 2. Effects of **32** at 4 × MIC on macromolecular synthesis in *E. coli TolC*. Controls: cerulenin (Cer), chloramphenicol (Cam), ciprofloxacin (Cipro), and rifampicin (Rif).

biosynthesis was observed (Figure 2). In this regard, it is also of interest that benzamidobenzoic acids, including compounds **2** and **3**, have been described in the context of antiinfective research. While compound **3** was shown to inhibit PqsD, an enzyme associated with the *Pseudomonas* quorum sensing system,[20] compounds **2** and **3** have been published as inhibitors of FabH, an enzyme involved in fatty acid synthesis.[21] Therefore, it can be supposed that the good antibacterial activity is due to an additional FabH inhibition.

As it is our aim to develop compounds which are less susceptible to bacterial resistance development, the sponta-

dx.doi.org/10.1021/jm400485e | J. Med. Chem. 2013, 56, 8332−8338

neous resistance frequencies in *E. coli TolC* were determined in vitro for compounds **28** and **32** at 2 × MIC. Importantly, a lower resistance frequency ($<4.5 \times 10^{-11}$) of both novel compounds compared to Rif (8.3×10^{-8}) was observed. One explanation for this remarkable observation could be the dual target effects of our compounds.

CONCLUSION

RNAP is an attractive antibacterial target, but due to emerging resistance, new types of RNAP inhibitors are urgently needed. For the discovery of those, we performed a flexible alignment with a series of selected RNAP inhibitors[8−12] and developed a pharmacophore model which is not focused on one particular binding site. Using this model, a virtual screening was performed, hit compounds were identified, and 11 of those subsequently experimentally validated. On the basis of three hits of one structural class, an optimization approach was performed, resulting in enhanced inhibitory potencies. Concerning the mechanism of RNAP inhibition, we could demonstrate that the new inhibitors prevent the PPI between σ^{70} and the RNAP core enzyme.

Determination of MIC values revealed that the best compounds are highly active against *E. coli TolC* and the Gram-positive pathogens *B. subtilis* as well as the clinically relevant *S. aureus*. The wild-type Gram-negative strains *P. aeruginosa* and *E. coli K12* were not affected, probably due to pharmacokinetic reasons.

Regarding the effects of our compounds on macromolecule synthesis in *E. coli TolC*, an inhibition of bacterial lipid biosynthesis was observed beside the reduced RNA formation. This highly interesting dual target effect could explain the good MIC values and the significantly lower resistance rate compared to the clinically used inhibitor Rif. These findings are presently further elucidated. In conclusion, we consider the new compounds promising for further development.

EXPERIMENTAL SECTION

Chemistry. All tested compounds have >95% chemical purity as measured by HPLC. Spectroscopic data for all compounds are provided in the SI.

Procedure for the Synthesis of the Acyl Chlorides Used for Amide Coupling Reaction. Benzoyl chlorides, if not commercially available, were obtained from the corresponding carboxylic acid via reaction with thionyl chloride (2.5 equiv) in CH_2Cl_2 in the presence of catalytic amounts of dimethylformamide (4 h reflux).

*General Procedure for the Synthesis of Methyl 2-Aminobenzoates **5b**, **21b−23b**, **25b**, **27b**, **29b**, and **30b**. Method A.* A solution of the appropriate 2-aminobenzoic acid (1 equiv) in MeOH was cooled to 0 °C followed by a dropwise addition of thionyl chloride (2.5 equiv). The mixture was refluxed for 24 h. After evaporation of the solvent and neutralization by addition of a saturated aqueous $NaHCO_3$ solution, the mixture was extracted with EtOAc and the combined organic layers were dried over $MgSO_4$. Purification by CC (*n*-hexane/EtOAc) provided the title compounds (yields, physical, and spectral data are reported in SI).

*General Procedure for the Synthesis of Methyl 2-Benzamidobenzoate Derivatives **1a−34a** (Amide Coupling Reaction). Method B.* Three different procedures were used to obtain the title compounds:

BI. The appropriate methyl 2-aminobenzoate (1 equiv) was added to a solution of the acyl chloride (1.2 equiv) in CH_2Cl_2 under a N_2 atmosphere. After the addition of TEA (2 equiv), the reaction mixture was stirred for 18 h at room temperature.

BII. The appropriate methyl 2-aminobenzoate (1 equiv) and a catalytic amount of DMAP were added to a suspension of the acyl chloride (1.5 equiv) in pyridine under a N_2 atmosphere. The reaction mixture was stirred for 18 h at room temperature, and 2 M HCl was added. The mixture was extracted with EtOAc, and the combined organic layers washed with saturated $NaHCO_3$ and dried over $MgSO_4$.

BIII. The appropriate methyl 2-aminobenzoate (1 equiv) and the acyl chloride (1.2 equiv) were dissolved in toluene and refluxed for 4 h (except for **5a** and **33a−34a**, which were refluxed for 18 or 72 h).

For purification, the solvent was removed under reduced pressure and the remaining solid suspended in MeOH (except for **5a** and **31a−32a**). After filtration, the precipitate was washed with MeOH to yield the pure compound.

For compounds **5a** and **31a−32a**, the purification step was performed by CC or preparative TLC.

*General Procedure for the Synthesis of 2-Benzamidobenzoate Derivatives **1−34**. Method C.* The methyl esters of the title compounds (**1a−34a**) were hydrolyzed with 5 M NaOH in THF/MeOH (2:1) at room temperature (18 h). The mixture was acidified by the addition of 1 M HCl and filtered, and the precipitate was washed with 1 M HCl to provide the title compounds. If the compound was not pure at this stage of the procedure, it was washed with MeOH and CH_2Cl_2 or was purified by CC or preparative TLC.

General Procedure for Suzuki Coupling. Method D. A mixture of the appropriate methyl bromo-2-benzamidobenzoate (1 equiv), phenylboronic acid (1.5 equiv), Cs_2CO_3 (3 equiv), and tetrakis-(triphenylphosphine)-palladium (0.01 equiv) in a degassed DME/water (1:1) solution was refluxed under a nitrogen atmosphere for 4 h. The reaction mixture was cooled to room temperature. The mixture was extracted with EtOAc. The combined organic layers were washed with 1 M HCl and dried over $MgSO_4$. The product was purified by CC or preparative TLC.

General Procedure for Ether Cleavage Using Boron Tribromide. Method E. To a solution of the appropriate methoxy substituted methyl 2-benzamidobenzoate derivative (1 equiv) in anhydrous CH_2Cl_2 at −78 °C (dry ice/acetone bath), boron tribromide (1 M in CH_2Cl_2, 6 equiv) was added dropwise. The reaction mixture was stirred for 18 h at room temperature under a nitrogen atmosphere. Water was added, and the aqueous layer was extracted with EtOAc. The combined organic layers were washed with brine and dried over $MgSO_4$. The product was purified by CC followed by preparative TLC.

Biology. *Transcription Assay.* Transcription assay was performed as described previously.[13,22] During the transcription time of 10 min, the substrate concentration as well as the enzyme activity were not limiting the transcription reaction. Consequently, the reaction process in our assay was linear.

Determination of IC_{50} Values. For the determination of IC_{50} values, three different concentrations of a compound were chosen (duplicate determination) in the linear range of the log dose response curve (20−80% inhibition) including concentrations above and below the IC_{50} value. The calculation of the IC_{50} value was performed by plotting the percent inhibition versus the concentration of inhibitor on a semilog plot. From this, the molar concentration causing 50% inhibition was calculated. At least three independent determinations were performed for each compound. Standard deviation was less than 20%.

Minimal Inhibitory Concentration (MIC) Determinations. These experiments were performed as described recently.[22] Given MIC values are means of two independent determinations (three if MIC <10 μg/mL) and are defined as the lowest concentration of compounds that reduced OD_{600} by ≥95%.

Determination of Resistance Frequencies. Defined amounts of *E. coli TolC* cells were incubated in LB in presence of the 2 × MIC of compounds **28** and **32** in parallel (16 h, 37 °C, 50 rpm, 0.5% DMSO). On each of the three following days, a fraction of each of the samples was supplemented with fresh compound containing LB followed by recultivation (conditions as before). The final cultures were plated on LB agar to select spontaneous resistant mutants. The bacterial start concentration which was needed to yield at least one colony on the plates was determined. The reciprocal value of this threshold was defined to be the resistance frequency. For **28** and **32**, no colonies

dx.doi.org/10.1021/jm400485e | J. Med. Chem. 2013, 56, 8332−8338

were detected at the highest possible bacterial start concentration, resulting in a resistance frequency $<4.5 \times 10^{-11}$.

Macromolecular Biosynthesis Assay. *E. coli TolC* was cultured in lysogeny broth (LB) medium. ^{3}H labeled precursors (1−1.25 μCi/mL) were added during the logarithmic growth phase and several min (3 min for uridine and thymidine, 5 min for acetic acid, 12 min for glutamine) before the addition of compound **32** and the controls chloramphenicol (Cam), cerulenin (Cer), ciprofloxacin (Cipro), and rifampicin (Rif) at four times their MICs. For DNA, RNA, and protein synthesis, 300 μL of the cultured bacteria were harvested 0 and 30 min after addition of the inhibitors and supplemented with 2 volumes of 10% TCA. After 45 min at 4 °C, the precipitates were collected and washed using 96-well glass fiber filter plates (Multiscreen GFB) (Millipore, Billerica, MA). After adding Optiphase Supermix (Perkin-Elmer, Waltham, MA), the quantification of radioactivity was performed using a Wallac MicroBeta TriLux system (Perkin-Elmer). For determination of lipid synthesis, cells were treated with $CHCl_3$/MeOH (1:1) and water, subsequently. The organic phase was collected, evaporated, redissolved in cyclohexane, and supplemented with Opti-Fluor O (Perkin-Elmer) before measuring the radioactivity in the MicroBeta TriLux.

ELISA-Based RNAP Assembly Assay. The procedure was performed as described by Hüsecken et al.[14]

Core/Holo Transcription Assay. The procedure was performed as described by Hüsecken et al.[14]

■ ASSOCIATED CONTENT

Ⓢ Supporting Information

Synthesis, compound characterization, and computational chemistry. This material is available free of charge via the Internet at http://pubs.acs.org.

■ AUTHOR INFORMATION

Corresponding Author

*Phone: +49 681 302 70300. Fax: +49 681 302 70308. E-mail: rwh@mx.uni-saarland.de or rolf.hartmann@helmholtz-hzi.de.

Author Contributions

The manuscript was written through contributions of all authors.

Notes

The authors declare no competing financial interest.

■ ACKNOWLEDGMENTS

We thank Jeannine Jung for determination of RNAP IC_{50} values and Jannine Ludwig for determination of MIC values.

■ ABBREVIATIONS USED

CC, column chromatography; FabH, β-ketoacyl-acyl carrier protein synthase III; LB, lysogeny broth; PPI, protein−protein interaction; RNAP, RNA polymerase; SD, standard deviation; TEA, triethylamine; TT, transcription/translation

■ REFERENCES

(1) Hooper, D. C.; DeMaria, A.; Limbago, B. M.; O'Brien, T. F.; McCaughey, B. Antibiotic resistance: how serious is the problem, and what can be done? *Clin. Chem.* **2012**, *58*, 1182−1186.

(2) Chopra, I. The 2012 Garrod Lecture: Discovery of Antibacterial Drugs in the 21st Century. *J. Antimicrob. Chemother.* **2013**, *68*, 496−505.

(3) Villain-Guillot, P.; Bastide, L.; Gualtieri, M.; Leonetti, J.-P. Progress in targeting bacterial transcription. *Drug Discovery Today* **2007**, *12*, 200−208.

(4) Ho, M. X.; Hudson, B. P.; Das, K.; Arnold, E.; Ebright, R. H. Structures of RNA polymerase−antibiotic complexes. *Curr. Opin. Struct. Biol.* **2009**, *19*, 715−723.

(5) Hardesty, J. S.; Juang, P. Fidaxomicin: a macrocyclic antibiotic for the treatment of *Clostridium difficile* infection. *Pharmacotherapy* **2011**, *31*, 877−886.

(6) Mariani, R.; Maffiolo, S. I. Bacterial RNA polymerase inhibitors: an organized overview of their structure, derivatives, biological activity and current clinical development status. *Curr. Med. Chem.* **2009**, *16*, 430−454.

(7) Chopra, I. Bacterial RNA polymerase: a promising target for the discovery of new antimicrobial agents. *Curr. Opin. Invest. Dr.* **2007**, *8*, 600−607.

(8) Arhin, F.; Bélanger, O.; Ciblat, S.; Dehbi, M.; Delorme, D.; Dietrich, E.; Dixit, D.; Lafontaine, Y.; Lehoux, D.; Liu, J.; McKay, G. A.; Moeck, G.; Reddy, R.; Rose, Y.; Srikumar, R.; Tanaka, K. S. E.; Williams, D. M.; Gros, P.; Pelletier, J.; Parr, T. R., Jr.; Far, A. R. A new class of small molecule RNA polymerase inhibitors with activity against rifampicin-resistant *Staphylococcus aureus*. *Bioorg. Med. Chem.* **2006**, *14*, 5812−5832.

(9) Artsimovitch, I.; Chu, C.; Lynch, A. S.; Landick, R. A new class of bacterial RNA polymerase inhibitor affects nucleotide addition. *Science* **2003**, *302*, 650−654.

(10) André, E.; Bastide, L.; Michaux-Charachon, S.; Gouby, A.; Villain-Guillot, P.; Latouche, J.; Bouchet, A.; Gualtiéri, M.; Leonetti, J.-P. Novel synthetic molecules targeting the bacterial RNA polymerase assembly. *J. Antimicrob. Chemother.* **2006**, *57*, 245−251.

(11) Villain-Guillot, P.; Gualtieri, M.; Bastide, L.; Roquet, F. o.; Martinez, J.; Amblard, M.; Pugniere, M.; Leonetti, J.-P. Structure−Activity Relationships of phenyl-furanyl-rhodanines as inhibitors of RNA polymerase with antibacterial activity on biofilms. *J. Med. Chem.* **2007**, *50*, 4195−4204.

(12) Larsen, S. D.; Hester, M. R.; Craig Ruble, J.; Kamilar, G. M.; Romero, D. L.; Wakefield, B.; Melchior, E. P.; Sweeney, M. T.; Marotti, K. R. Discovery and initial development of a novel class of antibacterials: Inhibitors of *Staphylococcus aureus* transcription/translation. *Bioorg. Med. Chem. Lett.* **2006**, *16*, 6173−6177.

(13) Haupenthal, J.; Hüsecken, K.; Negri, M.; Maurer, C. K.; Hartmann, R. W. Influence of DNA template choice on transcription and inhibition of *Escherichia coli* RNA polymerase. *Antimicrob. Agents Chemother.* **2012**, *56*, 4536−4539.

(14) Hüsecken, K.; Negri, M.; Fruth, M.; Boettcher, S.; Hartmann, R. W.; Haupenthal, J. Peptide-based investigation of the *Escherichia coli* RNA polymerase σ^{70}: core interface as target site. *ACS Chem. Biol.* **2013**, *8*, 758−766.

(15) Thornsberry, C.; Hill, B. C.; Swenson, J. M.; McDougal, L. K. Rifampin: spectrum of antibacterial activity. *Rev. Infect. Dis.* **1983**, *5*, 412−417.

(16) Bandow, J. E.; Brötz, H.; Hecker, M. *Bacillus subtilis* tolerance of moderate concentrations of Rifampin involves the sigma(B)-dependent general and multiple stress response. *J. Bacteriol.* **2002**, *184*, 459−467.

(17) Fowler, C. E.; Soothill, J. S.; Oakes, L. MICs of rifampicin and chloramphenicol for mucoid *Pseudomonas aeruginosa* strains are lower when human lactoferrin is present. *J. Antimicrob. Chemother.* **1997**, *40*, 877−879.

(18) Williams, K. J.; Piddock, L. J. Accumulation of rifampicin by *Escherichia coli* and *Staphylococcus aureus*. *J. Antimicrob. Chemother.* **1998**, *42*, 597−603.

(19) Irschik, H.; Gerth, K.; Höfle, G.; Kohl, W.; Reichenbach, H. The myxopyronins, new inhibitors of bacterial RNA synthesis from *Myxococcus fulvus* (*Myxobacterales*). *J. Antibiot.* **1983**, *36*, 1651−1658.

(20) Pistorius, D.; Ullrich, A.; Lucas, S.; Hartmann, R. W.; Kazmaier, U.; Müller, R. Biosynthesis of 2-alkyl-4(1*H*)-quinolones in *Pseudomonas aeruginosa*: potential for therapeutic interference with pathogenicity. *ChemBioChem* **2011**, *12*, 850−853.

(21) Nie, Z.; Perretta, C.; Lu, J.; Su, Y.; Margosiak, S.; Gajiwala, K. S.; Cortez, J.; Nikulin, V.; Yager, K. M.; Appelt, K.; Chu, S. Structure-based design, synthesis, and study of potent inhibitors of β-ketoacyl-acyl carrier protein synthase III as potential antimicrobial agents. *J. Med. Chem.* **2005**, *48*, 1596−1609.

(22) Sahner, J. H.; Groh, M.; Negri, M.; Haupenthal, J.; Hartmann, R. W. Novel small molecule inhibitors targeting the "switch region" of bacterial RNAP: structure-based optimization of a virtual screening hit. *Eur. J. Med. Chem.* **2013**, *65*, 223−231.